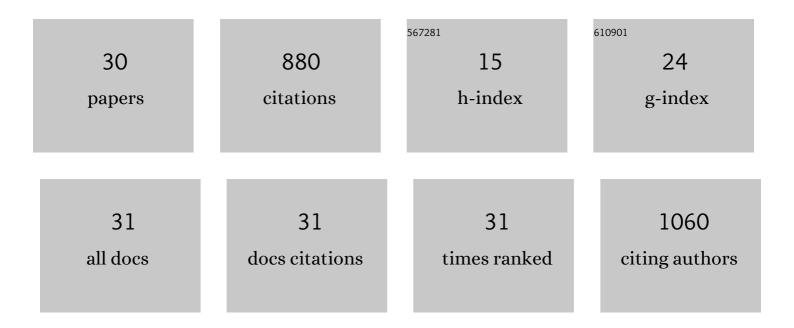


## List of Publications by Year in descending order

Source: https://exaly.com/author-pdf/4250212/publications.pdf Version: 2024-02-01



IÃ DOEN DALL

#	Article	IF	CITATIONS
1	Improving SAR Automatic Target Recognition Models With Transfer Learning From Simulated Data. IEEE Geoscience and Remote Sensing Letters, 2017, 14, 1484-1488.	3.1	161
2	EMISAR: an absolutely calibrated polarimetric L- and C-band SAR. IEEE Transactions on Geoscience and Remote Sensing, 1998, 36, 1852-1865.	6.3	99
3	Terahertz Imaging Systems With Aperture Synthesis Techniques. IEEE Transactions on Microwave Theory and Techniques, 2010, 58, 2027-2039.	4.6	95
4	Topography and penetration of the Greenland Ice Sheet measured with Airborne SAR Interferometry. Geophysical Research Letters, 2001, 28, 1703-1706.	4.0	61
5	Sea-Ice Deformation State From Synthetic Aperture Radar Imagery—Part I: Comparison of C- and L-Band and Different Polarization. IEEE Transactions on Geoscience and Remote Sensing, 2007, 45, 3610-3622.	6.3	47
6	Sea surface height determination in the Arctic using Cryosat-2 SAR data from primary peak empirical retrackers. Advances in Space Research, 2015, 55, 40-50.	2.6	46
7	The Danish SAR system: design and initial tests. IEEE Transactions on Geoscience and Remote Sensing, 1991, 29, 417-426.	6.3	42
8	Single and Multipolarimetric P-Band SAR Tomography of Subsurface Ice Structure. IEEE Transactions on Geoscience and Remote Sensing, 2016, 54, 2832-2845.	6.3	37
9	Volume changes of Vatnajökull ice cap, Iceland, due to surface mass balance, ice flow, and subglacial melting at geothermal areas. Geophysical Research Letters, 2005, 32, .	4.0	33
10	Wideband Dual-Polarization Microstrip Patch Antenna Array for Airborne Ice Sounder. IEEE Antennas and Propagation Magazine, 2012, 54, 98-107.	1.4	27
11	Response of Eyjafjallajökull, Torfajökull and Tindfjallajökull ice caps in Iceland to regional warming, deduced by remote sensing. Polar Research, 2011, 30, 7282.	1.6	25
12	Greenland ice velocity maps from the PROMICE project. Earth System Science Data, 2021, 13, 3491-3512.	9.9	23
13	A Polarimetric Coherence Method to Determine Ice Crystal Orientation Fabric From Radar Sounding: Application to the NEEM Ice Core Region. IEEE Transactions on Geoscience and Remote Sensing, 2019, 57, 8641-8657.	6.3	19
14	Characteristics of ice rises and ice rumples in Dronning Maud Land and Enderby Land, Antarctica. Journal of Glaciology, 2020, 66, 1064-1078.	2.2	19
15	Intercomparison and Validation of SAR-Based Ice Velocity Measurement Techniques within the Greenland Ice Sheet CCI Project. Remote Sensing, 2018, 10, 929.	4.0	18
16	SAR focusing of P-band ice sounding data using back-projection. , 2010, , .		16
17	Ice sheet anisotropy measured with polarimetric ice sounding radar. , 2010, , .		16
18	Direction-of-Arrival Estimation for Radar Ice Sounding Surface Clutter Suppression. IEEE Transactions on Geoscience and Remote Sensing, 2015, 53, 5170-5179.	6.3	16

JÃ, RGEN DALL

#	Article	IF	CITATIONS
19	Sea Ice Deformation State From Synthetic Aperture Radar Imagery—Part II: Effects of Spatial Resolution and Noise Level. IEEE Transactions on Geoscience and Remote Sensing, 2008, 46, 2197-2207.	6.3	14
20	Multichannel surface clutter suppression: East Antarctica P-band SAR ice sounding in the presence of grating lobes. Annals of Glaciology, 2014, 55, 9-21.	1.4	12
21	Synthetic Aperture Radar Data Processing on an FPGA Multi-core System. Lecture Notes in Computer Science, 2013, , 74-85.	1.3	10
22	The 20th century retreat of ice caps in Iceland derived from airborne SAR: W-Vatnajökull and N-Mýrdalsjökull. Earth and Planetary Science Letters, 2005, 237, 508-515.	4.4	9
23	Direction-of-Arrival Analysis of Airborne Ice Depth Sounder Data. IEEE Transactions on Geoscience and Remote Sensing, 2017, 55, 2239-2249.	6.3	9
24	SAR mapping of Burfellshraun: A terrestrial analog for recent volcanism on Mars. Journal of Geophysical Research, 2006, 111, .	3.3	5
25	300 GHz imaging with 8 meter stand-off distance and one-dimensional synthetic image reconstruction. Proceedings of SPIE, 2011, , .	0.8	5
26	Tomographic SAR analysis of subsurface ice structure in Greenland: First results. , 2013, , .		5
27	Estimation of Crystal Orientation Fabric from Airborne Polarimetric Ice Sounding Radar Data. , 2020, ,		4
28	On the Impact of Channel Imbalance on MIMO Radar Performance. , 2021, , .		3
29	Mutual Coupling and Channel Imbalance Calibration of Colocated MIMO Radars. IEEE Open Journal of Antennas and Propagation, 2022, 3, 511-522.	3.7	2
30	A mul ti-element THz imaging system. , 2010, , .		1